Starvation-induced NEDD4-mediated autophagy in BMSCs

CHENGYI LIU[1-3], SHUANG ZHANG[1-3], XIAOXIAN YUN[1], BO LI[1-3], XIAOMEI XU[1-3] and FUWEI LIN[1-3]

[1]Luzhou Key Laboratory of Oral and Maxillofacial Reconstruction and Regeneration, The Affiliated Stomatological Hospital of Southwest Medical University, Luzhou, Sichuan 646000, P.R. China; [2]Department of Oral Orthodontics, The Affiliated Stomatological Hospital of Southwest Medical University, Luzhou, Sichuan 646000, P.R. China; [3]School of Stomatology, Southwest Medical University, Luzhou, Sichuan 646000, P.R. China

Received March 17, 2025; Accepted December 19, 2025

DOI: 10.3892/br.2026.2105

Abstract. Autophagy regulates the osteogenic differentiation of bone marrow mesenchymal stem cells (BMSCs) and mediates BMSC-mediated bone remodeling under pathological conditions (such as osteoporosis and infectious bone defects). However, the regulatory mechanisms controlling autophagy in BMSCs remain unclear. Neural precursor cell-expressed developmentally down-regulated protein 4 (NEDD4) has been implicated in autophagy regulation. In the present study, autophagy was induced in BMSCs through serum starvation and NEDD4 expression was silenced using lentiviral short hairpin RNA. Quantitative real-time polymerase chain reaction, western blotting, and immunofluorescence were used to examine the expression of the autophagy-related molecules, microtubule-associated protein 1 light chain 3 (LC3) and Beclin-1, to explore the underlying molecular mechanisms. It was determined that BMSCs exhibited significant autophagy activation 30 min after starvation, accompanied by marked increases in NEDD4, LC3, and Beclin-1 at both mRNA and protein levels. NEDD4 knockdown significantly attenuated the upregulation of LC3 and Beclin-1 and prevented the starvation-induced decrease in phosphorylated mTOR. These results indicated that NEDD4 positively regulates autophagy in BMSCs, likely through the mTOR signaling pathway. In conclusion, the present study demonstrated that NEDD4 is essential for BMSC autophagy and may serve as an important target for therapies aimed at modulating BMSC function.

Correspondence to: Dr Fuwei Lin, Department of Oral Orthodontics, The Affiliated Stomatological Hospital of Southwest Medical University, 2 Jiangyang South Road, Luzhou, Sichuan 646000, P.R. China
E-mail: lfwxnykdkq@swmu.edu.cn

Abbreviations: BMSCs, bone marrow mesenchymal stem cells; DAPI, 4',6-diamidino-2-phenylindole; EBSS, Earle's balanced salt solution; LC3, light chain 3; MOI, multiplicity of infection; mTOR, mammalian target of rapamycin; NEDD4, neural precursor cell-expressed developmentally down-regulated protein 4; p-, phosphorylated; SD, standard deviation; TEM, transmission electron microscopy

Key words: autophagy, bone marrow mesenchymal stem cells, bone remodeling, NEDD4, serum starvation

Introduction

Bone remodeling is an ongoing and intricate physiological process essential for preserving bone integrity and functionality. It depends on the balance between osteoclast-mediated bone resorption and osteoblast-driven bone formation (1). Osteoporosis is defined by a disruption in the equilibrium between bone resorption and formation, resulting in diminished bone density and a heightened susceptibility to fractures (2). The compromised ability of bone marrow mesenchymal stem cells (BMSCs) to undergo osteogenic differentiation is a critical factor underlying the reduced capacity for bone formation (3). BMSCs are pivotal in bone formation during remodeling and repair. Research into conditions such as bone defects and osteoporosis focuses on guiding bone remodeling toward formation by modulating BMSCs (4). In the field of oral regenerative repair, BMSCs have demonstrated tremendous potential in promoting alveolar bone repair and regeneration. Numerous studies have shown that BMSCs significantly enhance the regeneration of alveolar bone defects whether used alone or in combination with materials such as fibrin glue or scaffolds (5,6). The use of BMSCs in periodontal bone tissue regeneration and repair has significant potential to enhance the scope of tooth movement and extend the applicability to orthodontic and dental interventions, ultimately delivering safer and more effective treatment alternatives for patients.

Autophagy plays an essential role in osteogenesis and periodontal bone tissue regeneration. Autophagy is a cellular self-degradation and recycling process in which damaged or excess organelles, proteins, and other macromolecules are enclosed in autophagosomes and eventually degraded within lysosomes (7). This mechanism supports cellular homeostasis and allows cells to manage stress conditions such as nutrient deprivation or oxidative stress, significantly impacting numerous physiological and pathological processes (8). Autophagy is integral to the development and progression of human diseases, with numerous studies highlighting its close association with various conditions (9); it suppresses early tumorigenesis but promotes survival in advanced cancer (10), contributes to neurodegeneration (for example Parkinson's disease) via defective protein/organelle

clearance (11), modulates cardiovascular injury outcomes (12), exacerbates metabolic disorders such as type 2 diabetes when impaired (13), and participates in host defense against pathogens (14). Research on cellular autophagy is crucial for understanding cell biology and disease mechanisms, potentially leading to novel therapeutic discoveries. Studies have shown that autophagy levels increase in a time-dependent manner during the osteogenic differentiation of BMSCs, highlighting its essential role in promoting osteogenesis (15,16). Specifically, autophagy activation promotes the differentiation of BMSCs into osteoblasts. Moreover, under conditions of nutrient deprivation or oxidative stress, autophagy can sustain osteoblast activity by clearing damaged mitochondria and proteins (17). Research has shown that hypoxic conditions in the local periodontal microenvironment caused by orthodontic treatments can induce autophagy, thereby affecting the remodeling of periodontal bone tissue (18). Therefore, understanding the mechanisms underlying autophagy in BMSCs holds substantial clinical and research value.

Autophagy progresses from initiation to autophagosome-lysosome fusion and the eventual degradation of cellular contents (19). The mammalian target of rapamycin (mTOR) pathway is a central regulator of cellular autophagy, orchestrating the autophagy process through diverse molecular mechanisms and signaling pathways. mTOR responds to various signals such as cellular nutritional status, energy levels, and growth factors to adjust the metabolism and growth of the cell (20). mTOR affects autophagy through downstream proteins such as neural precursor cell-expressed developmentally down-regulated protein 4 (NEDD4). NEDD4 consists of an N-terminal C2 domain, a C-terminal HECT domain, and two to four WW domains (21). Studies have shown that NEDD4 is essential for the survival of cranial neural crest cells and the development of craniofacial bones (22). Mice with *Nedd4* gene deletion were shown to exhibit notable craniofacial defects (23). Furthermore, osteoprogenitor cells lacking NEDD4 exhibited impaired osteogenic differentiation (24). Our preliminary research has also shown that NEDD4 knockout promotes osteogenic differentiation in BMSCs (25). Notably, the role that NEDD4 plays in autophagy has also attracted attention. NEDD4, an E3 ubiquitin ligase, facilitates protein degradation through ubiquitination. NEDD4 influences the stability and function of autophagy-related proteins, including light chain 3 (LC3) and Beclin-1, via direct or indirect ubiquitination. These proteins are recognized autophagy markers and exhibit increased expression levels during autophagic activity (26-29). Tumor cell research has shown that NEDD4 promotes autophagy and is associated with the mTOR signaling pathway (30). Meanwhile, our preliminary research revealed that NEDD4 knockout increased the expression of mTORC1 (25). mTORC1, a key element of the mTOR signaling pathway, was essential for autophagy regulation.

Based on these observations, it was hypothesized that NEDD4 expression in BMSCs promotes autophagy via the mTOR pathway. To test this hypothesis, autophagy was induced in BMSCs under starvation conditions and NEDD4 expression was modulated by lentiviral knockdown. The changes were then examined in autophagy (LC3 and Beclin-1 levels) and mTOR pathway activity in response to NEDD4 knockdown. Through this experimental design, the effect of NEDD4 on starvation-induced autophagy in BMSCs via mTOR was sought to be elucidated, and the potential of NEDD4 as a novel therapeutic target for conditions such as periodontal bone defects and osteoporosis was aimed to be determined.

Materials and methods

Animals. Male, 4-week-old Sprague-Dawley rats (n=8; body weight, 80-100 g) were obtained from the Experimental Animal Center of Southwest Medical University (Luzhou, China). The animals were housed under standard laboratory conditions with a controlled temperature of 20-26˚C, a relative humidity of 40-70%, a 12-h light/dark cycle, and *ad libitum* access to standard rodent chow and sterile drinking water. After euthanasia by carbon dioxide asphyxiation, femurs were dissected for BMSC extraction. For euthanasia, carbon dioxide (CO_2) was introduced into an uncharged chamber at a displacement rate of 30-70% of the chamber volume per minute, in accordance with the 2020 AVMA Guidelines. Death was confirmed by cessation of respiration and heartbeat, lack of corneal reflexes, and a secondary physical method (cervical dislocation). Ethical approval for the animal experiments was granted by the Ethics Committee of Southwest Medical University in Luzhou, Sichuan, China (approval no. 20221206-005).

Cell culture and identification. The rat femurs were dissected and rinsed with sterile phosphate-buffered saline (PBS; cat. no. 1001002; Gibco; Thermo Fisher Scientific, Inc. 3), and the soft tissues attached to the femurs were removed in a sterile biosafety cabinet. α-Minimum essential medium (α-MEM; cat no. 12561056; Gibco, Thermo Fisher Scientific, Inc.) containing 10% fetal bovine serum (FBS; cat. no. 10099141; Gibco;Thermo Fisher Scientific, Inc.) was used for cell culture.

The BMSC cell suspension was centrifuged at 1,000 x g at 4˚C for 5 min and then resuspended in α-MEM supplemented with 10% FBS, 100 μg/ml penicillin and 100 μg/ml streptomycin (cat. no. 15140122; Gibco; Thermo Fisher Scientific, Inc.), and incubated in a humidified atmosphere containing 5% CO_2 at 37˚C. After 48 h, the medium was replaced with fresh medium to remove non-adherent cells. When cell confluency reached 80%, the cells were passaged, and the passaged cells were designated as passage 1 (P1). Subsequent experiments were performed using third-passage cells (P3).

Flow cytometry was performed to detect the surface markers of P1 BMSCs (CD29, CD90, CD45, and CD34). The following primary antibodies were used to label the corresponding markers: FITC-conjugated anti-rat CD29 antibody (cat. no. 102206, dilution, 1:100; BioLegend, Inc.), PE-Cy7-conjugated anti-rat CD90 antibody (cat. no. 202517; dilution, 1:100; BioLegend, Inc.), PE-conjugated anti-rat CD34 antibody (cat no. 551387; dilution, 1:100; BD Pharmingen; BD Biosciences), and AF647-conjugated anti-rat CD45 antibody (cat. no. 160303; dilution, 1:100; BioLegend, Inc.). All primary antibodies were directly conjugated with fluorochromes (FITC, PE-Cy7, PE, and AF647 as reporter moieties); therefore, no secondary antibodies were required. Detection was performed using a direct immunofluorescence assay with a flow cytometer, and the fluorochrome-conjugated primary antibodies were excited at their respective optimal wavelengths to detect fluorescence signals. After incubation for 30 min at 4˚C in the

dark, the cells were analyzed using a fluorescence-activated cell sorter (FACSCalibur; BD Biosciences). Data acquisition and analysis were performed using FlowJo software (version 10.8.1; FlowJo LLC). The protocol for isolating and identifying BMSCs was consistent with previously described methods (31).

Multilineage differentiation induction and starvation-induced autophagy. P3 BMSCs were cultured in 6-well plates until cell confluence exceeded 80%, after which the medium was switched to either adipogenic or osteogenic induction medium, with the medium changed every three days. The adipogenic induction medium consisted of α-MEM supplemented with 10% FBS, 1 μM dexamethasone (cat. no. D8040), 0.5 mM 3-isobutyl-1-methylxanthine (IBMX; cat. no. II00101), 10 μg/ml insulin (cat. no. I8040), and 100 μM indomethacin (cat. no. II0100; all from Beijing Solarbio Science & Technology Co., Ltd.). The osteogenic induction medium consisted of α-MEM with 10% FBS, 10 mM β-glycerophosphate (cat. no. G9140), 50 μg/ml L-ascorbic acid-2-phosphate sesquimagnesium salt hydrate (cat. no. A8960-5G; Sigma-Aldrich; Merck KGaA), and 100 nM dexamethasone (cat. no. D8040; all from Beijing Solarbio Science & Technology Co., Ltd.). Cells were washed three times with PBS and fixed in 4% paraformaldehyde for 30 min at room temperature on the 14th day of adipogenic induction and the 21st day of osteogenic induction. Alizarin Red S (cat. no. G1452) and Oil Red O (cat. no. G1262; both from Beijing Solarbio Science & Technology Co., Ltd.) were used to stain osteogenically and adipogenically induced cells, respectively, according to the manufacturer's instructions.

Autophagy was induced by nutrient starvation. Nutrient deprivation using Earle's balanced salt solution (EBSS; cat. no. H2045) is a standard approach to trigger autophagy by acutely limiting amino acids and growth factors; this method is widely used to assess upstream regulators of autophagy. EBSS was therefore selected to induce autophagy in BMSCs (32,33). Briefly, P3 BMSCs in a logarithmic growth condition were switched to EBSS once confluence reached ~70%, marking time point 0 as the start of induction.

Lentiviral infection. Lentiviruses expressing short hairpin RNA (shRNA) targeting NEDD4 (sh-NEDD4) and a non-targeting control shRNA (sh-NC) were constructed using the GV493 lentiviral vector (hU6-MCS-CBh-gcGFP-IRES-puromycin; Shanghai GeneChem Co., Ltd.). Lentiviral packaging was performed using 293T cells (cat. no. SNL-015; Wuhan SunnCell Biotech Co., Ltd.) as the packaging cell line. For each 6-well plate transfection, 4 μg of lentiviral plasmids (sh-NEDD4 or sh-NC) were utilized, with lentiviral, packaging (psPAX2) and envelope (pMD2.G) plasmids mixed at a strict mass ratio of 4:3:1. The transfection was carried out in at 37˚C incubator supplemented with 5% CO_2 for 48 h consecutively. Culture supernatants harboring lentiviral particles were harvested at 48 and 72 h post-transfection, subjected to centrifugation at 1,000 x g for 20 min at 4˚C and filtration through a 0.45-μm filter membrane to eliminate cell debris, thus obtaining purified lentiviral particles. Following lentiviral transduction of BMSCs, the cells were cultured for an additional 72 h to ensure sufficient viral integration prior to initiating subsequent nutrient deprivation experiments. Puromycin (cat. no. P8230; Beijing Solarbio Science & Technology Co., Ltd.) was utilized for positive selection of stably transduced cell clones, with a selection concentration of 3.5 μg/ml and a maintenance concentration of 1.5 μg/ml during long-term subsequent culture. The specific target sequences of the shRNAs are detailed in Table I. For the transduction procedure, passage 3 (P3) BMSCs in the logarithmic growth phase were detached with trypsin and adjusted to a cell density of $5x10^4$ cells/ml. Each well of a 6-well plate was seeded with 1 ml of the cell suspension, after which the cells were co-incubated with lentivirus in the presence of HitransG P transduction enhancer for 16 h at 37˚C. Fresh growth medium was replenished at 24 h post-transduction. The multiplicity of infection (MOI) was determined using the formula: (virus titer x volume of virus added)/number of cells, and an optimal MOI of 50 was selected and applied in all experiments of this study.

Table I. shRNA target sequences used in this study.

shRNA ID	Accession	Target sequence (5'→3')
sh-NC	NM_012986	TTCTCCGAACGTGTCACGT
sh1	NM_012986	AGCCACAAATCAAGAGTTAAA
sh2	NM_012986	TTGGAAGGACCTACTACGTAA
sh3	NM_012986	CTGGATTGAGTTTGATGGTGA

sh-, short hairpin; NC, negative control.

Reverse transcription-quantitative polymerase chain reaction (RT-qPCR). Total RNA was isolated from cells using the TRIzol reagent (Invitrogen; Thermo Fisher Scientific, inc.) according to the manufacturer's instructions. cDNA synthesis was carried out with the PrimeScript Reverse Transcription Kit (Takara Bio, Inc.). RT-qPCR with SYBR Premix Ex Taq (Takara Bio, Inc.) was used to quantify the gene expression levels of NEDD4, LC3, and Beclin-1 (*Becn1*) with glyceraldehyde-3-phosphate dehydrogenase (GAPDH) as the reference gene. The thermocycling conditions were as follows: Initial denaturation at 95˚C for 30 sec, followed by 40 cycles at 95˚C for 5 sec and 60˚C for 30 sec; a melt-curve analysis was performed to confirm specificity. Relative expression was calculated using the $2^{-\Delta\Delta Cq}$ method (34). Primer sequences are provided in Table II.

Western blotting. Cellular protein was extracted with RIPA lysis buffer containing 1 mM phenylmethylsulfonyl fluoride (Beyotime Institute of Biotechnology) according to the manufacturer's instructions. The protein concentration was measured using a BCA assay kit (Beyotime Institute of Biotechnology). Western blotting was performed according to standard protocols (35). Specifically, equal amounts of total protein (20-30 μg per lane) were separated by 12% SDS-PAGE and transferred to PVDF membranes (0.45 μm). Membranes were blocked with 5% bovine serum albumin (BSA; cat. no. SW3015; Beijing Solarbio Science & Technology Co., Ltd.) in TBST containing 0.1% Tween-20 for 1 h at room temperature, then incubated overnight at 4˚C with primary antibodies:

Table II. Primer sequences of the measured genes.

Genes	Sequence of primers (5'→3')
GAPDH	R: TAGCCCAGGATGCCCTTTAGT
	F: CCCCCAATGTATCCGTTGTG
LC3B	R: GCCGAAGGTTTCTTGGGAGG
	F: TTGGTCAAGATCATCCGGCG
Beclin-1	R: AATTGTCCGCTGTGCCAGATATG
	F: GCTCAAGAGTGTAGAGAACCAGA
NEDD4	R: GCCAGACCTATGCCAGCTAT
	F: GCTTTCGGAGGACGAGGTAT

LC3, light chain 3; NEDD4, neural precursor cell-expressed developmentally down-regulated protein 4; R, reverse; F, forward.

GAPDH [cat. no. 2118; 1:3,000-1:5,000; Cell Signaling Technology (CST)], LC3B (cat. no. ab192890; 1:1,000; Abcam), Beclin-1 (cat. no. 3495; 1:1,000; CST), NEDD4 (cat. no. 2740; 1:1,000; CST), total mTOR (cat. no. 2983; 1:1,000; CST), and phospho-mTOR (Ser2448; cat. no. 5536; 1:1,000; CST). After washing, membranes were incubated with HRP-conjugated secondary antibodies (anti-rabbit IgG, cat. no. 7074; anti-mouse IgG, 7076; each at 1:5,000; CST) for 1 h at room temperature. Bands were visualized using an enhanced chemiluminescent substrate (SuperSignal West Pico PLUS; cat. no. 34580; Thermo Fisher Scientific, Inc.) and imaged on a digital chemiluminescence system. Within each composite figure panel, proteins were probed on the same membrane (using membrane cutting or strip-and-reprobe) unless otherwise indicated. Densitometric analysis of the blots was performed using ImageJ software (version 1.8.0_172; National Institutes of Health).

Immunofluorescence. Cells were seeded into 24-well plates at a density of $1x10^4$ cells per well. After adherence, cells were fixed with 4% paraformaldehyde for 15 min at room temperature, permeabilized with 0.5% Triton X-100 for 15 min at room temperature, and blocked with 5% BSA for 60 min at room temperature. Cells were then incubated overnight at 4˚C with an anti-LC3 primary antibody (cat. no. ab192890; 1:1,000; Abcam). The following day, cells were washed three times with PBS and incubated for 1 h at room temperature with an Alexa Fluor 594-conjugated goat anti-rabbit secondary antibody (cat. no. 31460; Thermo Fisher Scientific, Inc.) at a dilution of 1:1,000 in 5% BSA/PBS for 1 h at room temperature. Nuclei were counterstained with 4',6-diamidino-2-phenylindole (DAPI; cat. no. C0065; Beijing Solarbio Science & Technology Co., Ltd.) at a dilution of 1:5,000 in PBS for 10 min at room temperature. After washing with PBS, the cells were observed under a fluorescence microscope (Olympus Corporation). These immunocytochemical procedures followed previously published protocols (35).

Transmission electron microscopy (TEM). Autophagic vesicles (AVs) were visualized using TEM. Cells were collected by gentle scraping and initially fixed in 3% glutaraldehyde (cat. no. G5882; Sigma-Aldrich; Merck KGaA) in 0.1 M phosphate buffer (pH 7.4) at 4˚C for 2 h, followed by post-fixation with 1% osmium tetroxide (cat. no. 201030; Sigma-Aldrich; Merck KGaA) at 4˚C for 30 min. Cells were dehydrated through a graded ethanol series, embedded in Epon resin (cat. no. 45345; Sigma-Aldrich; Merck KGaA), and ultrathin sections with a thickness of 50 nm were prepared. The sections were stained with 2% uranyl acetate (cat. no. S9062-5; RuiTaibio) at room temperature for 15 min, followed by lead citrate (cat. no. 17800; Electron Microscopy Sciences) at room temperature for 10 min. Subcellular structures were examined using a JEM-2000EX transmission electron microscope (JEOL, Ltd.).

Statistical analysis. Data processing and visualization were performed using GraphPad Prism (version 9.0; GraphPad Software; Dotmatics). All experiments were conducted in triplicate (n=3). Results are presented as the mean ± standard deviation (SD). One-way ANOVA was used to evaluate group differences. Following one-way ANOVA, Tukey's multiple-comparison post hoc test was applied for pairwise comparisons. A two-sided α value of 0.05 was considered the threshold for statistical significance; P-values <0.05 were considered to indicate a statistically significant difference.

Results

Culture and identification of BMSCs. Cells were extracted from rat femurs using whole bone marrow adherent culture techniques. After passaging, the cells exhibited a uniform fibroblast-like morphology and were arranged in a vortex pattern (Fig. 1A). Multilineage differentiation potential was observed. On day 21 of osteogenic induction, Alizarin Red S staining revealed numerous orange-red calcium nodules (Fig. 1B). Oil Red O staining after 14 days of adipogenic induction showed the presence of red lipid droplets, demonstrating the adipogenic potential of the cultured cells (Fig. 1C). Flow cytometric analysis indicated high expression of mesenchymal stem cell markers CD90 (98.73%) and CD29 (95.99%), whereas hematopoietic stem cell markers CD34 and CD45 were minimally expressed (0.3 and 0.05%, respectively), consistent with mesenchymal stem cell characteristics (Fig. 1D). These findings verify the successful isolation and culture of rat BMSCs.

Autophagy induction and expression of autophagy-related genes. Autophagy in BMSCs was induced by EBSS starvation, and cells were collected at specific time points. RT-qPCR analysis showed that the mRNA expression of NEDD4 and autophagy-related genes LC3 and Beclin-1 gradually increased, peaking at 30 min post-induction, and then decreased by 1 h (Fig. 2A). Western blot analysis showed that NEDD4 protein levels, along with autophagy markers LC3-II and Beclin-1, were elevated in BMSCs following EBSS starvation (with a maximum expression at ~30 min; Fig. 2B and C). Immunofluorescent staining further confirmed autophagy induction in BMSCs (Fig. 2D). LC3 was mainly expressed in the cytoplasm, and the fluorescence intensity of LC3 increased during the first 30 min of starvation. After 1 and 2 h, LC3 fluorescence remained strong, but the number of cells in the field of view decreased significantly and cell morphology changed. By 2 h, numerous cells exhibited pronounced shrinkage.

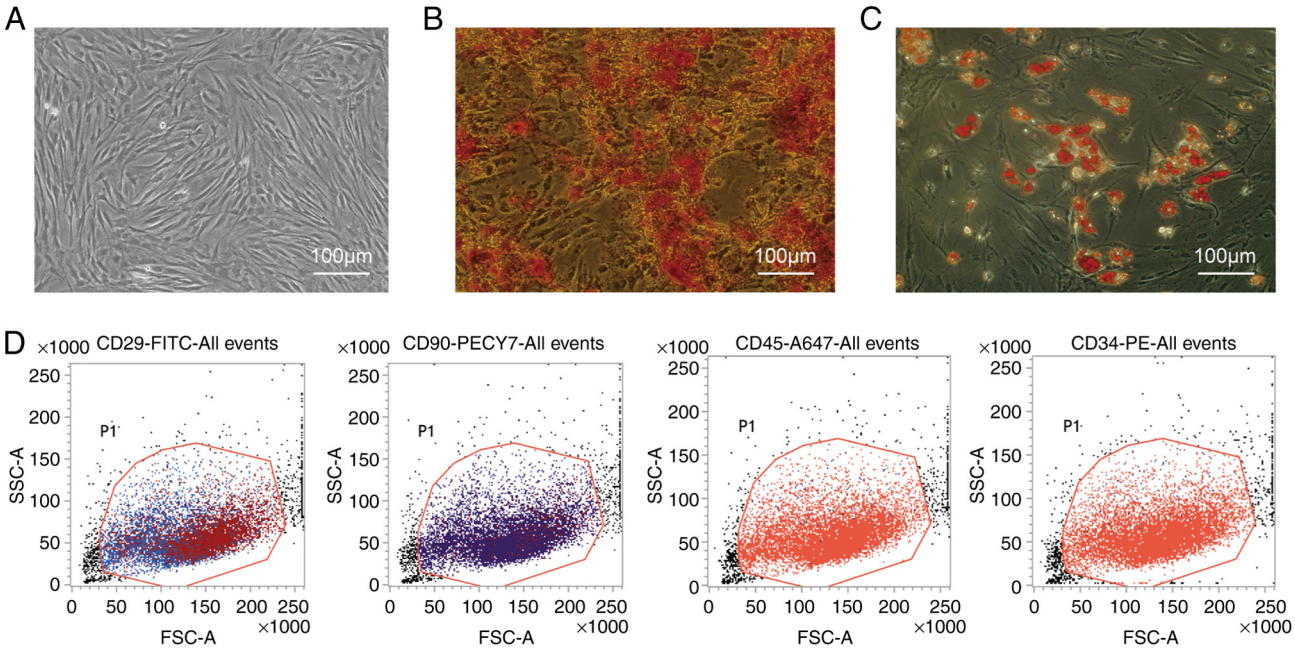

Figure 1. Culture and identification of BMSCs. (A) Representative light microscopy image showing the fibroblast-like morphology of third-generation (P3) BMSCs. (B) Alizarin Red S staining indicates mineralized calcium nodules after 21 days of osteogenic induction. (C) Oil Red O staining displays red lipid droplets in BMSCs after 14 days of adipogenic induction. (D) Flow cytometric analysis confirms BMSC identity based on high expression of CD29 and CD90, and low expression of CD34 and CD45. BMSCs, bone marrow mesenchymal stem cells.

TEM was employed to evaluate the formation of AVs among different groups. The results showed that there was a tendency for AV accumulation after starvation induction, reflecting autophagy induction, and the 30-min starvation group exhibited significant accumulation (Fig. 3). In addition, morphological changes such as nuclear shrinkage, fragmentation, and irregular edges were observed in cells 1 h after starvation, indicating the progression to adverse cellular conditions or apoptosis (consistent with excessive stress). Collectively, these results indicated that BMSCs undergo significant autophagy after 30 min of EBSS induction, which may be related to increased NEDD4 expression.

Knockdown of NEDD4 inhibits autophagy in BMSCs. Lentivirus-mediated NEDD4 knockdown was performed in BMSCs to investigate the role of NEDD4 in autophagy. The optimal infection condition was achieved using HitransG P with an MOI of 50 (Fig. 4A). Successful infection was further confirmed by puromycin selection, with optimal selection efficiency observed at a puromycin concentration of 3.5 μg/ml (Fig. 4B). RT-qPCR analysis revealed that among three shRNA sequences assessed, the sh3 sequence produced the most effective silencing of the NEDD4 gene. Therefore, the sh3 virus was selected for use in subsequent experiments (Fig. 4C).

Upon EBSS starvation, NEDD4-knockdown BMSCs exhibited a marked reduction in autophagy compared with controls. NEDD4 knockdown significantly blunted the starvation-induced increases in LC3 and Beclin-1 expression, keeping them below baseline levels (Fig. 5A). Immunofluorescent staining of LC3 (Fig. 5B) further demonstrated that autophagy was markedly suppressed in NEDD4-deficient cells: LC3 puncta formation and intensity were significantly lower in the sh-NEDD4 + EBSS group than in the EBSS (starvation only) group. These results indicated that NEDD4 is necessary for the full autophagic response in BMSCs under starvation, suggesting that NEDD4 mediates or positively regulates autophagy in BMSCs.

Possible association between NEDD4 and the mTOR pathway in the regulation of autophagy. The role of NEDD4 in autophagy in BMSCs was investigated by examining the mTOR pathway. Western blot analyses were used to assess mTOR activation status (p-mTOR) as well as autophagy markers, with and without NEDD4 knockdown (Fig. 6). The results showed that starvation (EBSS) led to increased protein levels of NEDD4, LC3-II, and Beclin-1, accompanied by a notable reduction in the level of p-mTOR, indicating suppression of mTOR activity during autophagy induction. When NEDD4 was knocked down, this trend was reversed. p-mTOR levels were restored (reaching higher levels than in starved control cells), while the levels of LC3-II and Beclin-1 were lower (consistent with the inhibition of autophagy). These results suggest that NEDD4 may activate autophagy at least in part by inhibiting the mTOR signaling pathway. In other words, NEDD4 acts upstream to negatively regulate mTOR during autophagy. This finding aligns with previous findings on the role of mTOR as a negative regulator of autophagy (30). In our prior research, it was observed that an increase in osteogenic differentiation markers in BMSCs was associated with improved bone-forming capability when autophagy was inhibited (25), suggesting a possible link between autophagy and osteogenesis. The present study identified NEDD4 as an upstream regulator of mTOR in BMSCs, offering novel insights into the molecular mechanisms governing BMSC autophagy and its potential impact on bone remodeling.

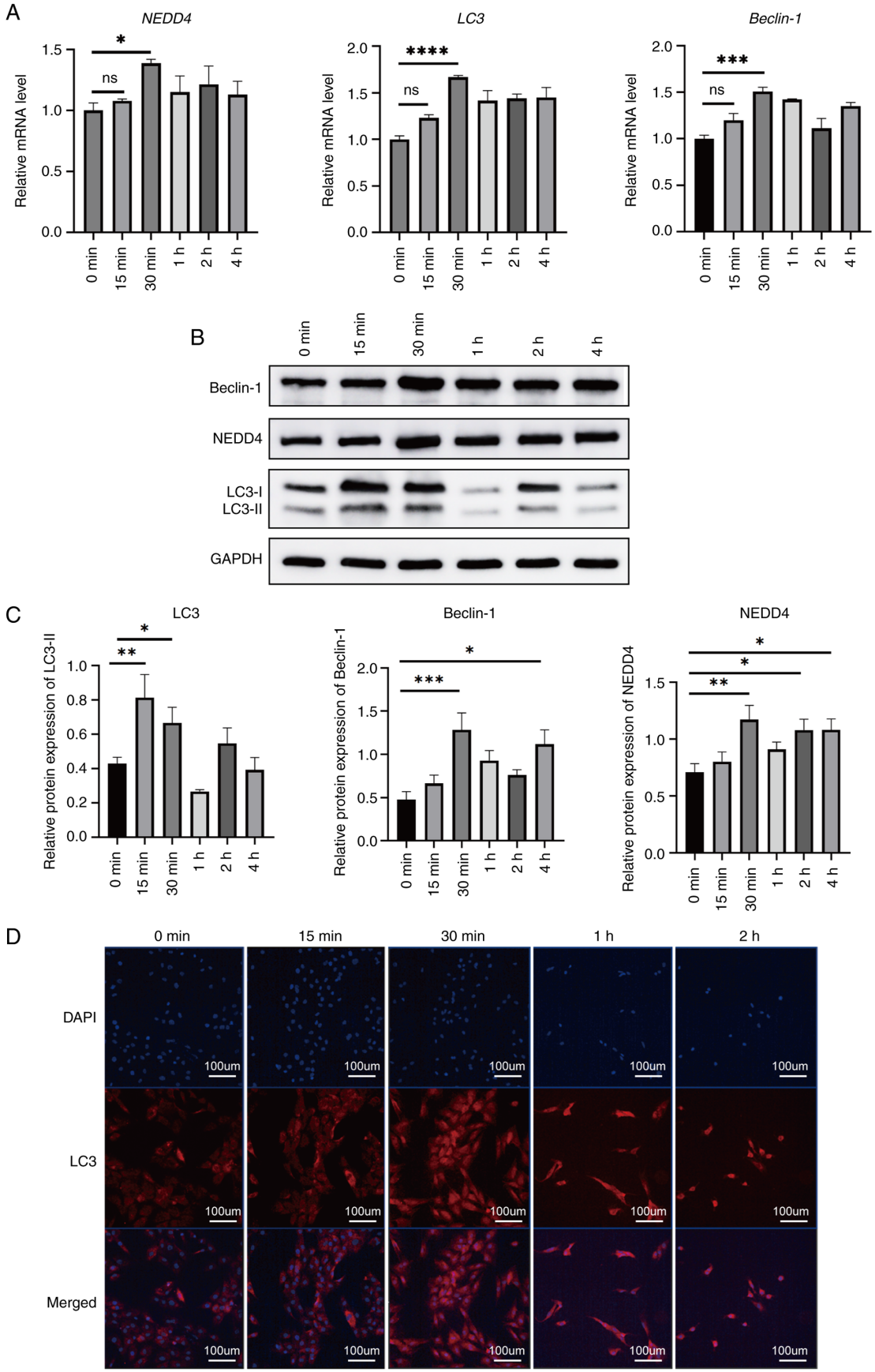

Figure 2. Time-course of autophagy induction in BMSCs following EBSS starvation. (A) RT-qPCR analysis of NEDD4, LC3, and Beclin-1 mRNA levels at 0, 15, 30 min, and 1, 2, 4 h post-starvation. (B and C) A representative western blot image and quantification of autophagy-related proteins NEDD4, LC3-I and -II, and Beclin-1 over time. (D) Representative immunofluorescent images showing LC3 (red) localization in the cytoplasm of BMSCs after starvation. Nuclei were counterstained with DAPI (blue). Scale bar, 100 μm. Data are presented as the mean ± SD (n=3). *P≤0.05, **P≤0.01, ***P≤0.001 and ****P≤0.0001. BMSCs, bone marrow mesenchymal stem cells; EBSS, Earle's balanced salt solution; RT-qPCR, reverse transcription-quantitative polymerase chain reaction; NEDD4, neural precursor cell-expressed developmentally down-regulated protein 4; LC3, light chain 3; DAPI, 4',6-diamidino-2-phenylindole; ns, not significant.

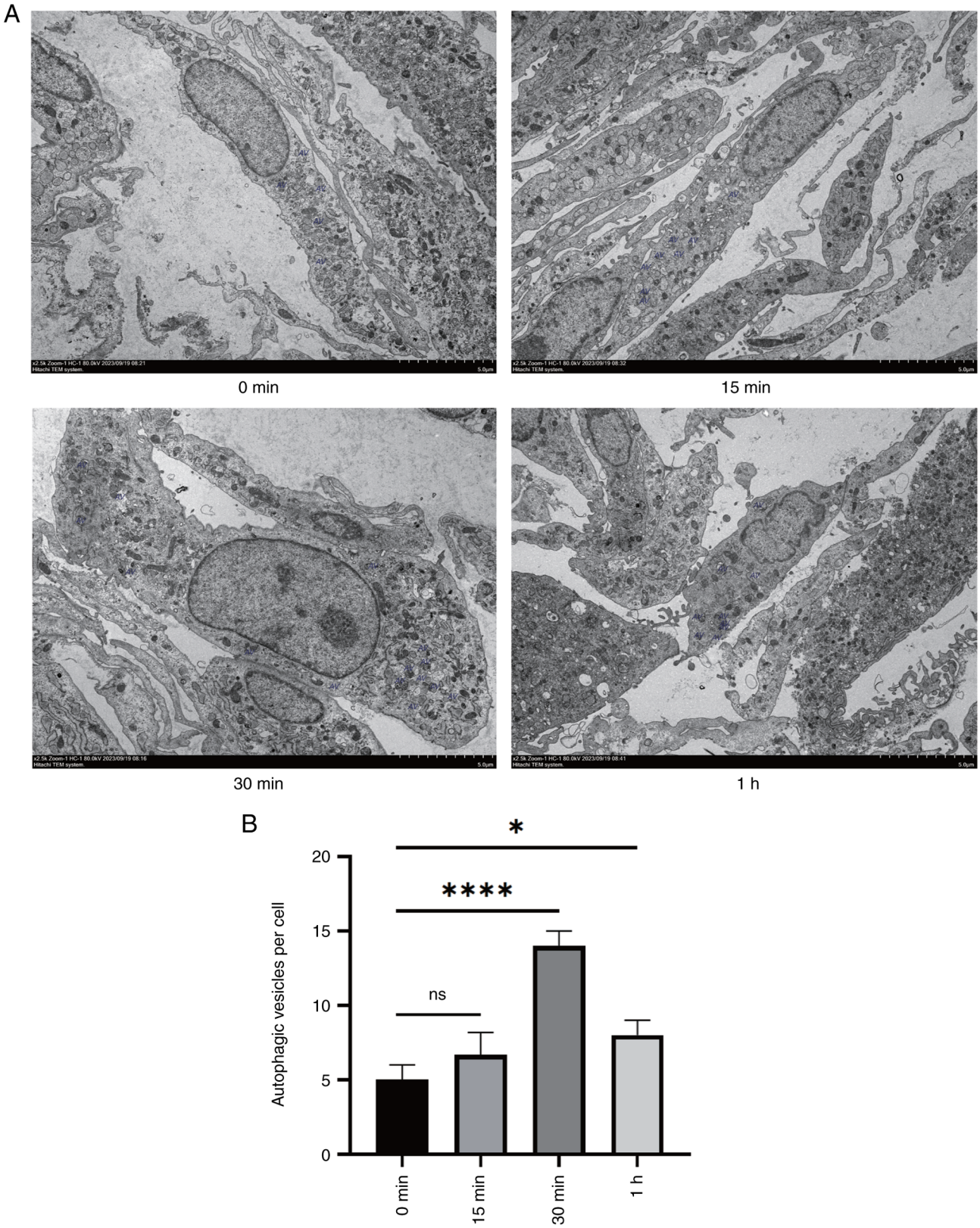

Figure 3. Ultrastructural observation of autophagy in BMSCs using TEM. (A) Representative TEM images of cellular autophagy at different time points. (B) Quantitative analysis of cellular autophagic vesicles at different time points. Data are presented as mean ± SD (n=3). *P≤0.01 and ****P≤0.0001. BMSCs, bone marrow mesenchymal stem cells; TEM, transmission electron microscopy; ns, not significant.

Discussion

The present study investigated the involvement of NEDD4 in BMSC autophagy. Our experimental findings demonstrated that NEDD4 is essential for the initiation and maintenance of autophagy in BMSCs. Through culturing of rat BMSCs, autophagy induction via starvation, and NEDD4 knockdown experiments, it was found that NEDD4 significantly influences

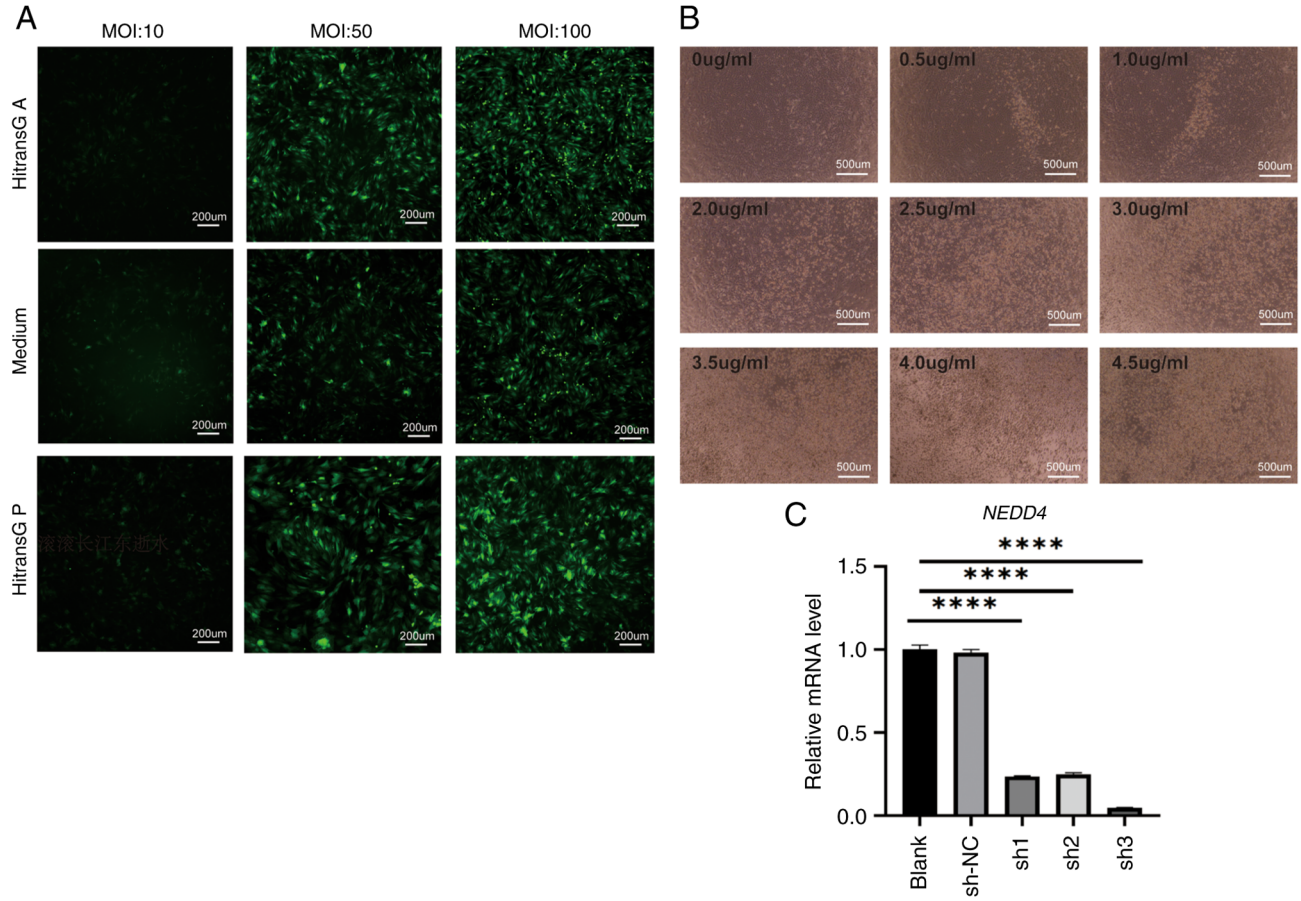

Figure 4. Optimization of lentiviral infection for NEDD4 knockdown in BMSCs. (A) Immunofluorescence imaging showing infection efficiency (MOI) with or without HitransG enhancers. (B) Cell morphology after puromycin selection at different concentrations. The optimal concentration is 3.5 μg/ml. (C) RT-qPCR results showing knockdown efficiency of three shRNA sequences targeting *NEDD4*; sh3 was selected for subsequent experiments. Data are shown as mean ± SD (n=3). ****P≤0.0001. NEDD4, neural precursor cell-expressed developmentally down-regulated protein 4; BMSCs, bone marrow mesenchymal stem cells; MOI, multiplicity of infection; RT-qPCR, reverse transcription-quantitative polymerase chain reaction; shRNA or sh-, short hairpin; NC, negative control.

the expression of autophagy-related genes and regulates this process through interactions with the mTOR signaling pathway. The findings offer novel insights into how NEDD4 and autophagy regulate BMSC function.

In the present study, autophagy was induced by EBSS starvation. RT-qPCR and western blot analyses indicated elevated Beclin-1 and LC3 expression following starvation induction, suggesting enhanced autophagic activity due to their essential roles in autophagy (36). Beclin-1 and LC3 expression are typically associated with autophagic activity. However, an increase in these proteins alone is insufficient to confirm autophagy, as such changes may reflect the initiation of autophagy rather than its completion. LC3, Beclin-1, and p62 are among the most well-known core autophagy proteins (37). To fully evaluate autophagy, measuring p62 levels, which typically decrease when autophagic flux increases, would be informative and p62 will be assessed in future experiments.

RT-qPCR and western blot analyses also revealed a marked increase in NEDD4 expression in BMSCs after 30 min of EBSS starvation-induced autophagy. NEDD4 expression was revealed to be positively associated with autophagy-related genes LC3 and Beclin-1, suggesting its role as a positive regulator of autophagy in BMSCs. NEDD4 is suggested to promote cell survival during stress (such as nutrient deprivation) by supporting autophagy.

Regarding the starvation duration, various time points (0-4 h) were assessed and it was found that BMSCs maintained acceptable viability up to ~30 min of starvation. After 1 h of starvation, cells exhibited contraction, rounding, and some cell detachment, with reduced cell density. TEM at 1 h revealed nuclear shrinkage, fragmentation, and irregular nuclear edges, indicating that prolonged starvation could initiate apoptotic changes. Starvation is known to activate autophagy as an adaptive response to help cells maintain energy balance by degrading and recycling intracellular components. However, prolonged starvation can trigger apoptosis. Autophagy and apoptosis, while distinct, have complex interrelationships that can be synergistic, mutually inhibitory, or even interconvertible under different conditions (38,39). Some studies suggest cells can undergo apoptosis and autophagy simultaneously (40,41). In our experiments, after 15 min of starvation, autophagy markers had begun to increase (as determined by RT-qPCR and western blotting) but not to the extent observed at 30 min, indicating that 15 min may have been insufficient for robust autophagy induction. Based on our comprehensive autophagy assessments (molecular and ultrastructural), 30 min of EBSS starvation was selected as the optimal induction duration for subsequent experiments.

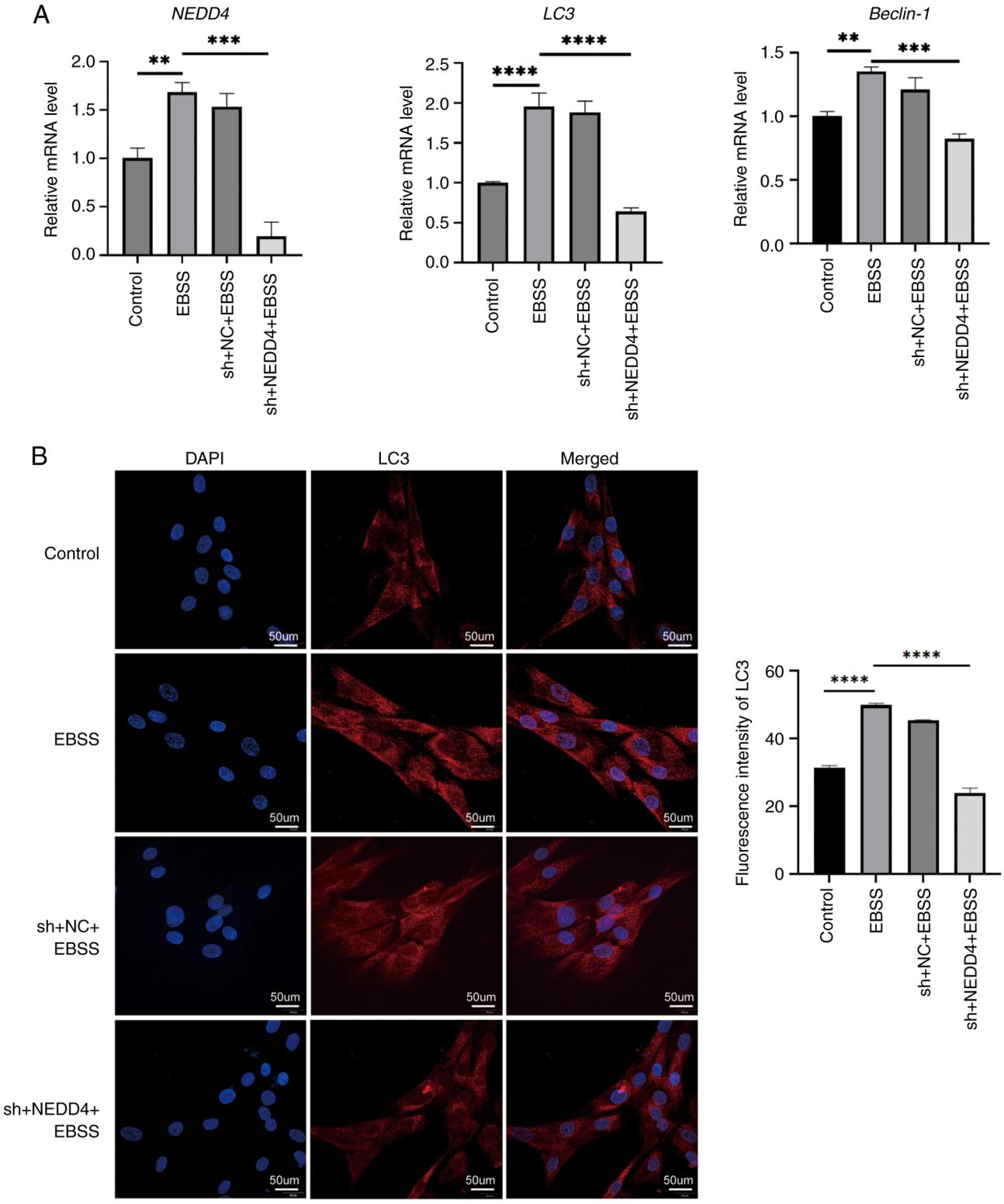

Figure 5. NEDD4 knockdown impairs starvation-induced autophagy in BMSCs. (A) RT-qPCR analysis of NEDD4, LC3 and Beclin-1 mRNA expression under control, EBSS, sh-NC + EBSS, and sh-NEDD4 + EBSS conditions. (B) Representative LC3 immunofluorescent images and quantification. LC3 puncta are markedly reduced in the NEDD4 knockdown group. Scale bar, 50 μm. Data are expressed as mean ± SD (n=3). **P≤0.01, ***P≤0.005 and ****P≤0.0001. NEDD4, neural precursor cell-expressed developmentally down-regulated protein 4; BMSCs, bone marrow mesenchymal stem cells; RT-qPCR, reverse transcription-quantitative polymerase chain reaction; LC3, light chain 3; EBSS, Earle's balanced salt solution; sh-, short hairpin; NC, negative control.

The experiments in the present study showed that knocking down NEDD4 significantly reduced the expression of LC3 and Beclin-1 in starved BMSCs. This finding aligns with that of Sun *et al* (27), who demonstrated that stable NEDD4 knockdown in A549 lung cancer cells inhibited starvation- and rapamycin-induced autophagy, thereby reducing LC3-II levels. In addition, NEDD4 directly interacted with LC3. These results indicated that NEDD4 is not only a positive regulator

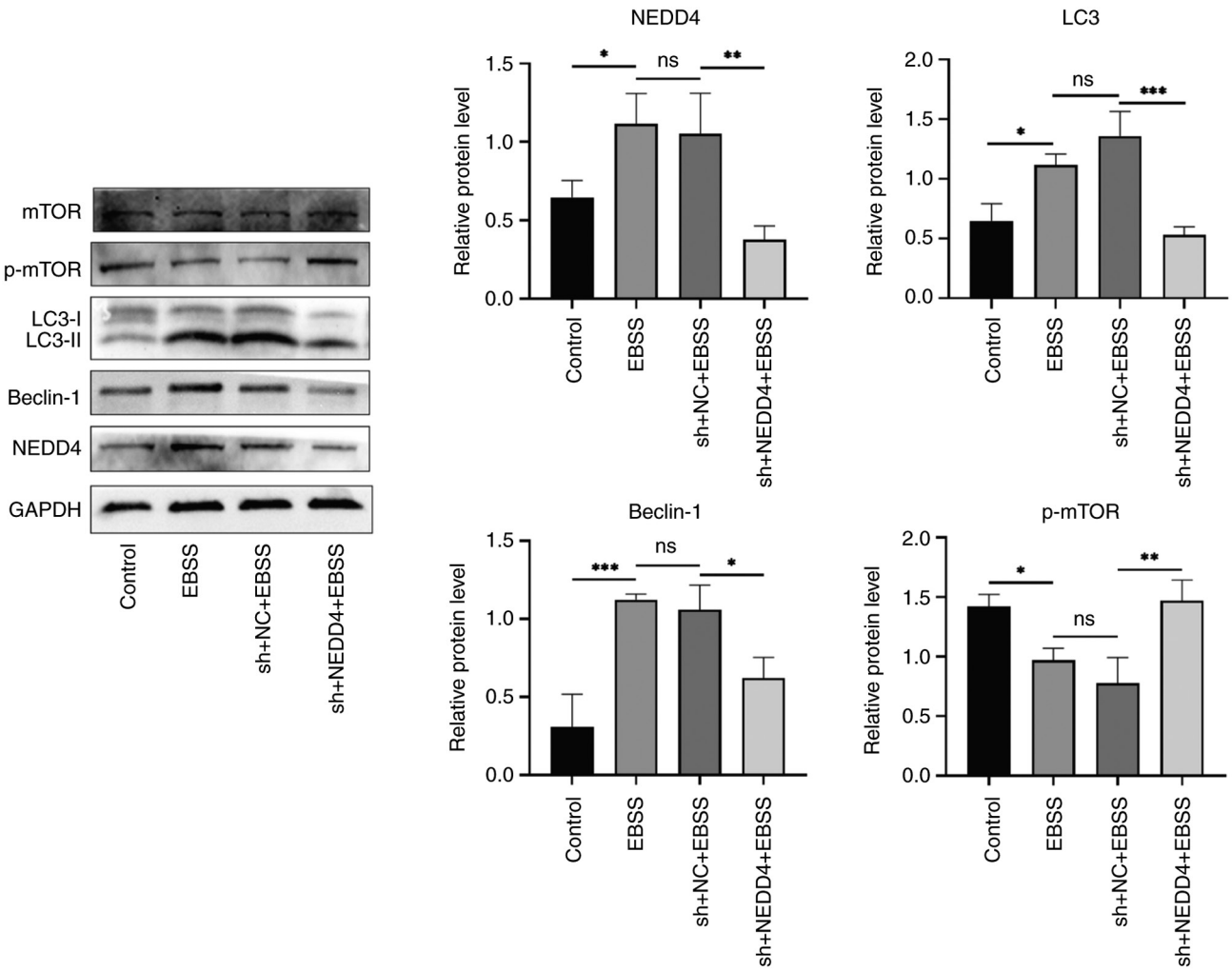

Figure 6. Effects of NEDD4 knockdown on autophagy markers and mTOR signaling. A representative western blot image and quantification of LC3-II, Beclin-1, total mTOR, and p-mTOR in BMSCs under EBSS treatment, with and without NEDD4 knockdown. NEDD4 knockdown reverses EBSS-induced reduction in p-mTOR, indicating mTOR reactivation. Data are shown as mean ± SD (n=3). *P≤0.01, **P≤0.005, ***P≤0.0001. Proteins shown within the panel were detected on the same membrane (cut by molecular weight) unless otherwise indicated. NEDD4, neural precursor cell-expressed developmentally down-regulated protein 4; mTOR, mammalian target of rapamycin; p-, phosphorylated; BMSCs, bone marrow mesenchymal stem cells; EBSS, Earle's balanced salt solution; sh-, short hairpin; NC, negative control.

of autophagy but is also essential for proper execution of the autophagic process.

A potential mechanism underlying NEDD4-mediated autophagy, was further investigated. mTOR is a well-established negative regulator of autophagy, suppressing autophagy under nutrient-rich conditions (42,43). Moreover, mTOR is a crucial regulator of osteogenic differentiation in mesenchymal stem cells such as stem cells from apical papilla, BMSCs, and periodontal ligament stem cells (44-47). In the experiments of the present study, EBSS-induced autophagy led to increased expression of NEDD4 and autophagy-related proteins (LC3-II and Beclin-1), along with a notable reduction in p-mTOR, indicating suppressed mTOR activity and enhanced autophagy. When NEDD4 was knocked down, p-mTOR levels were restored (signifying reactivation of mTOR), and autophagy (LC3-II and Beclin-1 levels) was inhibited. This suggests that NEDD4 may activate the autophagy program by inhibiting the mTOR signaling pathway. This interpretation is consistent with the well-known role of mTOR in autophagy regulation (30). In our prior research, it was observed that increased expression of osteogenic differentiation markers in BMSCs was associated with improved bone formation capacity (25). Other research indicates a potential link between suppressed autophagy and enhanced osteogenesis, although the exact mechanism remains to be explored (48). Thus, the present study identified NEDD4 as an upstream regulator of mTOR, offering novel insights into the molecular mechanisms connecting BMSC autophagy and bone remodeling.

In addition, it is acknowledged that further mechanistic validation is needed. Only nutrient starvation was employed to induce autophagy. Using specific autophagy modulators (such as rapamycin to inhibit mTOR or chloroquine to block autophagy flux) could strengthen the conclusions. In future studies, such modulators are planned to be used to further verify the role of NEDD4. Moreover, the present study design did not include a 'rescue' experiment (restoring NEDD4 expression after knockdown) to fulfill molecular causation criteria, nor were assays such as co-immunoprecipitation performed to test for direct interactions (for example between NEDD4 and components of the mTOR pathway) or ubiquitination assays

conducted to confirm the E3 ligase activity of NEDD4 on autophagy-related substrates. These experiments are beyond the scope of the present study and will be addressed in future research. Nevertheless, by combining our results with previous findings that NEDD4 promotes autophagy in other cell types (27), compelling evidence that NEDD4 acts as an upstream regulator of autophagy in BMSCs is provided. As a further step, ALP staining and mineralization assays (such as Alizarin Red S staining) could be employed in future work to directly evaluate how changes in NEDD4 expression or autophagy levels affect the osteogenic differentiation of BMSCs. These follow-up studies will help clarify the relationship between autophagy induced by NEDD4 and osteogenesis.

In summary, the present study revealed an important role for NEDD4 in regulating autophagy in BMSCs. By establishing *in vitro* BMSC models with NEDD4 knockdown, it was demonstrated that NEDD4 depletion impairs autophagy. The limited osteogenic differentiation of BMSCs is a key factor in reduced bone formation; the results of the present study suggest that NEDD4 (via autophagy activation through mTOR inhibition) could potentially enhance the osteogenic capacity of BMSCs. This positions NEDD4 as a promising therapeutic target for conditions such as osteoporosis. Future studies will further investigate the interplay between NEDD4-regulated autophagy and BMSC osteogenesis *in vivo*.

Acknowledgements

Not applicable.

Funding

The present study was funded by a grant from the Luzhou Science and Technology Plan Project (grant no. 2020-JYJ-40), the Natural Science Foundation of Southwest Medical University (grant no. 2021ZKMS020), the Tutor Group Capacity Improvement Project of The Affiliated Stomatological Hospital of Southwest Medical University (grant no. 2022DS16), and the Sichuan College Students Innovation and Entrepreneurship Training Program (grant no. S202210632170).

Availability of data and materials

The data generated in the present study may be requested from the corresponding author.

Authors' contributions

CL and FL conceived and designed the study. CL and XY carried out the methodology design and performed data analysis using software. SZ and XX conducted the formal analysis. BL was responsible for data curation and investigation. CL and XY wrote the original draft. FL and XX reviewed and edited the manuscript. CL and FL confirm the authenticity of all the raw data. All authors read and approved the final manuscript.

Ethics approval and consent to participate

Ethical approval for the animal experiments was granted by the Ethics Committee of Southwest Medical University, Luzhou, Sichuan, China (approval no. 20221206-005). All animal procedures were conducted in accordance with institutional guidelines, the National Research Council's Guide for the Care and Use of Laboratory Animals (8th ed.), and the AVMA Guidelines for the Euthanasia of Animals (2020).

Patient consent for publication

Not applicable.

Competing interests

The authors declare that they have no competing interests.

References

1. Wang L, You X, Zhang L, Zhang C and Zou W: Mechanical regulation of bone remodeling. Bone Res 10: 16, 2022.
2. Zhang G, Kang Y, Dong J, Shi D, Ziang Y, Gao H, Lin Z, Wei X, Ding R, Fan B, *et al*: Fluffy hybrid nanoadjuvants for reversing the imbalance of osteoclastic and osteogenic niches in osteoporosis. Bioact Mater 39: 354-374, 2024.
3. Liu F, Yuan L, Li L, Yang J, Liu J, Chen Y, Zhang J, Lu Y, Yuan Y and Cheng J: S-sulfhydration of SIRT3 combats BMSC senescence and ameliorates osteoporosis via stabilizing heterochromatic and mitochondrial homeostasis. Pharmacol Res 192: 106788, 2023.
4. Trompet D, Melis S, Chagin AS and Maes C: Skeletal stem and progenitor cells in bone development and repair. J Bone Miner Res 39: 633-654, 2024.
5. Shahnaser S, Sheikhi M, Hashemibeni B, Mousavi AS and Soltani P: Comparison of autogenous bone graft and tissue-engineered bone graft in alveolar cleft defects in canine animal models using digital radiography. Indian J Dent Res 31: 118-123, 2020.
6. Zhang L, Wang P, Mei S, Li C, Cai C and Ding Y: In vivo alveolar bone regeneration by bone marrow stem cells/fibrin glue composition. Arch Oral Biol 57: 238-244, 2012.
7. Mizushima N and Komatsu M: Autophagy: Renovation of cells and tissues. Cell 147: 728-741, 2011.
8. Mizushima N and Levine B: Autophagy in human diseases. N Engl J Med 383: 1564-1576, 2020.
9. Klionsky DJ, Petroni G, Amaravadi RK, Baehrecke EH, Ballabio A, Boya P, Bravo-San Pedro JM, Cadwell K, Cecconi F, Choi AMK, *et al*: Autophagy in major human diseases. EMBO J 40: e108863, 2021.
10. Amaravadi RK, Kimmelman AC and White E: Recent insights into the function of autophagy in cancer. Genes Dev 30: 1913-1930, 2016.
11. Menzies FM, Fleming A and Rubinsztein DC: Compromised autophagy and neurodegenerative diseases. Nat Rev Neurosci 16: 345-357, 2015.
12. Lavandero S, Chiong M, Rothermel BA and Hill JA: Autophagy in cardiovascular biology. J Clin Invest 125: 55-64, 2015.
13. Jung HS, Chung KW, Won Kim J, Kim J, Komatsu M, Tanaka K, Nguyen YH, Kang TM, Yoon KH, Kim JW, *et al*: Loss of autophagy diminishes pancreatic beta cell mass and function with resultant hyperglycemia. Cell Metab 8: 318-324, 2008.
14. Huang J and Brumell JH: Autophagy in immunity against intracellular bacteria. Curr Top Microbiol Immunol 335: 189-215, 2009.
15. Su Z, Chen D, Huang J, Liang Z, Ren W, Zhang Z, Jiang Q, Luo T and Guo L: Isoliquiritin treatment of osteoporosis by promoting osteogenic differentiation and autophagy of bone marrow mesenchymal stem cells. Phytother Res 38: 214-230, 2024.
16. Zeng C, Wang S, Chen F, Wang Z, Li J, Xie Z, Ma M, Wang P, Shen H and Wu Y: Alpinetin alleviates osteoporosis by promoting osteogenic differentiation in BMSCs by triggering autophagy via PKA/mTOR/ULK1 signaling. Phytother Res 37: 252-270, 2023.
17. Liu Y, Lin S, Xu Z, Wu Y, Wang G, Yang G, Cao L, Chang H, Zhou M and Jiang X: High-performance hydrogel-encapsulated engineered exosomes for supporting endoplasmic reticulum homeostasis and boosting diabetic bone regeneration. Adv Sci (Weinh) 11: e2309491, 2024.

18. Wang M, Zhang L, Lin F, Zheng Q, Xu X and Mei L: Dynamic study into autophagy and apoptosis during orthodontic tooth movement. Exp Ther Med 21: 430, 2021.
19. Xu HM and Hu F: The role of autophagy and mitophagy in cancers. Arch Physiol Biochem 128: 281-289, 2022.
20. Ceccariglia S, Cargnoni A, Silini AR and Parolini O: Autophagy: A potential key contributor to the therapeutic action of mesenchymal stem cells. Autophagy 16: 28-37, 2020.
21. Ingham RJ, Gish G and Pawson T: The Nedd4 family of E3 ubiquitin ligases: Functional diversity within a common modular architecture. Oncogene 23: 1972-1984, 2004.
22. Wiszniak S, Harvey N and Schwarz Q: Cell autonomous roles of Nedd4 in craniofacial bone formation. Dev Biol 410: 98-107, 2016.
23. Wiszniak S, Kabbara S, Lumb R, Scherer M, Secker G, Harvey N, Kumar S and Schwarz Q: The ubiquitin ligase Nedd4 regulates craniofacial development by promoting cranial neural crest cell survival and stem-cell like properties. Dev Biol 383: 186-200, 2013.
24. Jeon SA, Lee JH, Kim DW and Cho JY: E3-ubiquitin ligase NEDD4 enhances bone formation by removing TGFβ1-induced pSMAD1 in immature osteoblast. Bone 116: 248-258, 2018.
25. Li B, Zhang S, Yun X, Liu C, Xiao R, Lu M, Xu X and Lin F: NEDD4's effect on osteoblastogenesis potential of bone mesenchymal stem cells in rats concerned with PI3K/Akt pathway. Differentiation 141: 100830, 2025.
26. Luo M, Ye L, Chang R, Ye Y, Zhang Z, Liu C, Li S, Jing Y, Ruan H, Zhang G, *et al*: Multi-omics characterization of autophagy-related molecular features for therapeutic targeting of autophagy. Nat Commun 13: 6345, 2022.
27. Sun A, Wei J, Childress C, Shaw JH IV, Peng K, Shao G, Yang W and Lin Q: The E3 ubiquitin ligase NEDD4 is an LC3-interactive protein and regulates autophagy. Autophagy 13: 522-537, 2017.
28. Xie W, Jin S and Cui J: The NEDD4-USP13 axis facilitates autophagy via deubiquitinating PIK3C3. Autophagy 16: 1150-1151, 2020.
29. Xie W, Jin S, Wu Y, Xian H, Tian S, Lie DA, Guo Z and Cui J: Auto-ubiquitination of NEDD4-1 Recruits USP13 to facilitate autophagy through deubiquitinating VPS34. Cell Rep 30: 2807-2819.e4, 2020.
30. Li Y, Zhang L, Zhou J, Luo S, Huang R, Zhao C and Diao A: Nedd4 E3 ubiquitin ligase promotes cell proliferation and autophagy. Cell Prolif 48: 338-347, 2015.
31. Farahzadi R, Fathi E, Mesbah-Namin SA and Vietor I: Granulocyte differentiation of rat bone marrow resident C-kit^{+} hematopoietic stem cells induced by mesenchymal stem cells could be considered as new option in cell-based therapy. Regen Ther 23: 94-101, 2023.
32. Mizushima N, Yoshimori T and Levine B: Methods in mammalian autophagy research. Cell 140: 313-326, 2010.
33. Klionsky DJ, Abdel-Aziz AK, Abdelfatah S, Abdellatif M, Abdoli A, Abel S, Abeliovich H, Abildgaard MH, Abudu YP, Acevedo-Arozena A, *et al*. Guidelines for the use and interpretation of assays for monitoring autophagy (4th edition)[1]. Autophagy 17: 1-382, 2021.
34. Livak KJ and Schmittgen TD: Analysis of relative gene expression data using real-time quantitative PCR and the 2(-Delta Delta C(T)) method. Methods 25: 402-408, 2001.
35. Farahzadi R, Valipour B, Anakok OF, Fathi E and Montazersaheb S: The effects of encapsulation on NK cell differentiation potency of C-kit-hematopoietic stem cells via identifying cytokine profiles. Transpl Immunol 77: 101797, 2023.
36. Vicente GP, Della Salda L and Strefezzi RF: Beclin-1 and LC3B expression in canine mast cell tumours: An immuno-ultrastructural and immunohistochemical study of autophagy. Vet Q 44: 1-15, 2024.
37. Su S, Wu Y, Wang D and Hai J: Inhibition of excessive autophagy and mitophagy mediates neuroprotective effects of URB597 against chronic cerebral hypoperfusion. Cell Death Dis 9: 733, 2018.
38. Biswas U, Roy R, Ghosh S and Chakrabarti G: The interplay between autophagy and apoptosis: Its implication in lung cancer and therapeutics. Cancer Lett 585: 216662, 2024.
39. Remadevi V, Jaikumar VS, Vini R, Krishnendhu B, Azeez JM, Sundaram S and Sreeja S: Urolithin A, induces apoptosis and autophagy crosstalk in oral squamous cell carcinoma via mTOR/AKT/ERK1/2 pathway. Phytomedicine 130: 155721, 2024.
40. Zhu Y, Wang H, Wang J, Han S, Zhang Y, Ma M, Zhu Q, Zhang K and Yin H: Zearalenone Induces apoptosis and cytoprotective autophagy in chicken granulosa cells by PI3K-AKT-mTOR and MAPK signaling pathways. Toxins (Basel) 13: 199, 2021.
41. Li S, Xu B, Luo Y, Luo J, Huang S and Guo X: Autophagy and apoptosis in rabies virus replication. Cells 13: 183, 2024.
42. Kim J, Kundu M, Viollet B and Guan KL: AMPK and mTOR regulate autophagy through direct phosphorylation of Ulk1. Nat Cell Biol 13: 132-141, 2011.
43. Zhang Y, Vasheghani F, Li YH, Blati M, Simeone K, Fahmi H, Lussier B, Roughley P, Lagares D, Pelletier JP, *et al*: Cartilage-specific deletion of mTOR upregulates autophagy and protects mice from osteoarthritis. Ann Rheum Dis 74: 1432-1440, 2015.
44. Chen M, Jing D, Ye R, Yi J and Zhao Z: PPARβ/δ accelerates bone regeneration in diabetic mellitus by enhancing AMPK/mTOR pathway-mediated autophagy. Stem Cell Res Ther 12: 566, 2021.
45. Tanaka Y, Sonoda S, Yamaza H, Murata S, Nishida K, Hama S, Kyumoto-Nakamura Y, Uehara N, Nonaka K, Kukita T and Yamaza T: Suppression of AKT-mTOR signal pathway enhances osteogenic/dentinogenic capacity of stem cells from apical papilla. Stem Cell Res Ther 9: 334, 2018.
46. Zhao X, Sun W, Guo B and Cui L: Circular RNA BIRC6 depletion promotes osteogenic differentiation of periodontal ligament stem cells via the miR-543/PTEN/PI3K/AKT/mTOR signaling pathway in the inflammatory microenvironment. Stem Cell Res Ther 13: 417, 2022.
47. Jiang Z, Huang H, Luo L and Jiang B: The role of autophagy on osteogenesis of dental follicle cells under inflammatory microenvironment. Oral Dis 31: 928-940, 2025.
48. Zheng J, Gao Y, Lin H, Yuan C and Zhi K: Corrigendum to 'Enhanced autophagy suppresses inflammation-mediated bone loss through ROCK1 signaling in bone marrow mesenchymal stem cells' [Cells Dev. 167 (2021) 203687]. Cells Dev 176: 203867, 2023.